Published OnlineFirst October 16, 2017; DOI: 10.1158/0008-5472.CAN-17-0720

Tumor and Stem Cell Biology

Cancer Research

Administering xCT Inhibitors Based on Circadian Clock Improves Antitumor Effects

Fumiyasu Okazaki[1], Naoya Matsunaga[2,3], Kengo Hamamura[4], Kayoko Suzuki[1], Takaharu Nakao[3], Hiroyuki Okazaki[5], Masahiko Kutsukake[1], Shiro Fukumori[1], Yasuhiro Tsuji[1], and Hideto To[1]

Abstract

Clock genes encoding transcription factors that regulate circadian rhythms may inform chronomodulated chemotherapy, where time-dependent dose alterations might affect drug efficacy and reduce side effects. For example, inhibiting the essential cystine transporter xCT with sulfasalazine induces growth arrest in cancer cells. Although the anticancer effects of sulfasalazine have been studied extensively, its effects on transcriptional control of xCT expression have not been studied. Here, we show that sulfasalazine administration during the period of increased xCT expression improves its anticancer effects and that the *Clock* gene itself induces xCT expression and regulates its circadian rhythm. Our findings highlight the clinical potential of chronomodulated chemotherapy and the importance of xCT-mediated transcriptional regulation in the utility of such strategies. *Cancer Res; 77(23); 6603–13. ©2017 AACR.*

Introduction

The circadian clock system controls various biological functions in mammals. The master pacemaker of the mammalian clock is located in the suprachiasmatic nuclei of the hypothalamus (1). Circadian rhythms are controlled by the interplay of the interconnected components of transcriptional–translational feedback loops. Brain and muscle Arnt-like 1 (Bmal1) and circadian locomotor output cycles kaput (Clock) heterodimer enhances the transcription of cryptochrome (*Cry*) and period (*Per*), which, in turn, act as repressors through the interaction with the Bmal1/Clock complex, forming a negative feedback loop and inhibiting their own expression (2–4). This mechanism leads to a periodically repeated activation/repression of clock-controlled gene expression in peripheral tissues and tumor tissues as well (5).

Chronomodulated chemotherapy is based on the adjustment of applied drug dose according to the 24-hour variations of pharmacodynamic or pharmacokinetic factors, approximately 24-hour cycles in the physiologic processes that have been observed in humans, bacteria, and plants (6, 7). Chronotherapy can maximize the effectiveness or minimize the side effects of therapies by administrating the selected drug at specific time points depending on the patients' circadian rhythms (8). Chronomodulated chemotherapy demonstrates increased efficacy and reduced toxicity, because clock genes regulate a number of genes involved in the determination of drug pharmacodynamics and pharmacokinetics parameters (9, 10).

xCT is a plasma membrane cystine transporter involved in the regulation of glutathione (GSH) metabolism, and xCT inhibitors reduce GSH levels (11, 12). GSH is an important antioxidant, and its increased levels in cancer cells may lead to the development of chemotherapy and radiotherapy resistance (13, 14). In contrast, GSH depletion induces the sensitivity of tumor cells to anticancer drugs (15, 16). Therefore, xCT-mediated cystine uptake is induced in cancer cells, allowing them to develop anticancer drug resistance (17). In addition, the reduction of xCT expression leads to tumor growth arrest. Sulfasalazine, an xCT inhibitor, has recently attracted attention as a potential novel anticancer drug that is able to affect cancer cells and drug-resistant cancer cells, such as cancer stem–like cells (CSC), and has anticancer effects in combination therapy. A growing body of evidence suggests that sulfasalazine may represent a new anticancer drug with increased efficacy, which may lead to a complete eradication of cancer (18–21).

Chronotherapy may reduce the time required for the development of a new drug, because only the dosing time of the existing medications needs to be changed, which can lead to therapeutic improvements. In addition, the regulation of xCT expression and the mechanism of action of sulfasalazine have not been elucidated. Determining the mechanisms regulating xCT expression is important for the potential development of new anticancer therapies and for elucidating the role of xCT in cancer cells and CSCs.

Therefore, the aims of this study were to investigate the transcriptional regulation of *xCT* expression by clock genes and to explore the administration time-dependent effects of sulfasalazine on cancer cells.

Materials and Methods

Animals and cells

Seven-week-old male BALB/c or ICR mice (Sankyo Labo Service Corporation, Inc.) were housed under a standard light/dark cycle (light phase: 7:00–19:00) at temperature of 24 ± 1°C and

[1]Department of Medical Pharmaceutics, Faculty of Pharmaceutical Sciences, University of Toyama, Toyama, Japan. [2]Department of Glocal Healthcare Science, Faculty of Pharmaceutical Sciences, Kyushu University, Fukuoka, Japan. [3]Department of Pharmaceutics, Faculty of Pharmaceutical Sciences, Kyushu University, Fukuoka, Japan. [4]Department of Chemical Pharmacology, Daiichi University of Pharmacy, Fukuoka, Japan. [5]Department of Molecular Biology, Daiichi University of Pharmacy, Fukuoka, Japan.

Corresponding Author: F. Okazaki, University of Toyama, 2630 Sugitani, Toyama 930-0194, Japan. Phone: 81-76-415-8814; Fax: 81-76-434-7584; E-mail: fokazaki@pha.u-toyama.ac.jp

doi: 10.1158/0008-5472.CAN-17-0720

Published OnlineFirst October 16, 2017; DOI: 10.1158/0008-5472.CAN-17-0720

60 ± 10% humidity with *ad libitum* access to food and water. Colon 26 and S180 cells were obtained from the Cell Resource Center for Biomedical Research, Tohoku University (Sendai, Japan) in 2011 and 2012, respectively. Colon 26 and S180 cells were maintained in RPMI 1640 supplemented with 10% FBS at 37°C in a humidified atmosphere with 5% CO_2. The cell lines were authenticated by the cell bank using short tandem repeat–PCR analysis, and the cells were used within 3 months, from the frozen stock. Aliquots (25 μL) containing 5×10^5 viable colon 26 and S180 cells were injected into the right hind footpads of BALB/c and ICR mice, respectively. Mice bearing tumors were euthanized after the tumor size reached approximately 200 mm^3. Tumor volume was estimated according to the following formula: tumor volume (mm^3) = $4\pi xyz/3$, where 2x, 2y, and 2z represent three perpendicular diameters of the tumor. All experiments were performed in accordance with the Guide for the Care and Use of Laboratory Animals distributed by the U.S. National Institutes of Health.

RNA interference

Synthetic siRNA precursor molecules corresponding to mouse *Bmal1* (Silencer Select si-Bmal1; Cat. No. 4390771, ID: s62621), *Clock* (Silencer Select si-Clock; Cat. No. 4390771, ID: s64069), and siRNA-negative control molecules (Silencer Select Negative control No. 1; Cat. No. 4390843) were obtained from Thermo Fisher Scientific. Si-Bmal1, si-Clock, and negative control siRNA (final concentration, 5 nmol/L) were reverse transfected into colon 26 cells using Lipofectamine RNAiMAX (Thermo Fisher Scientific).

qRT-PCR analysis

Total mRNA was extracted using RNAiso Plus (TaKaRa Bio Inc.), and cDNA was synthesized with the PrimeScript RT reagent Kit with gDNA Eraser (TaKaRa Bio Inc.). Real-time PCR analyses were performed using KOD SYBR qPCR Mix (TOYOBO) with StepOnePlus (Thermo Fisher Scientific). All gene expression levels were normalized to those of the housekeeping gene *β-actin*. The mean values of the lowest gene expression levels, si-control group, or control group were set to 1.

Construction of reporter vectors

The 5′ flanking region of the mouse *xCT* gene (from −2,855 to −2,683; +1 indicates exon 1 of *xCT*) was amplified from murine DNA using KOD-plus-Neo (TOYOBO). PCR was performed using forward primer 5′-GAGGTACCAGATGCCATAGTGCTGTGA-CAC-3′ (KpnI) and the reverse primer 5′-GAAAGCTTTGC-TAAAGGTAACAGCCCCATG-3′ (HindIII). PCR products were purified and ligated into the pGL4.28 Basic vector (*xCT*-Luc). The sequence of the E-box (−2,716 to −2,711 bp) in *xCT*-Luc was mutated using a QuikChange site–directed mutagenesis kit (Agilent Technologies).

To construct *ClockΔ19* expression vector, total RNA was obtained from Clock-mutant mouse liver. Total RNA was converted to cDNA using ReverTra Ace (TOYOBO). The exon region of the mouse *Clock* gene was amplified from liver cDNA using Elongase Enzyme mix (Thermo Fisher Scientific). PCR was performed using the forward primer 5′-ATAGATATCATGGTGTT-TACCGTAAGCTGTA-3′ (EcoRV) and reverse primer 5′-ATACTC-GAGACCCTTCCAAGGTCCAGCCACAGTAG-3′ (XhoI). PCR products were purified and ligated into a pcDNA3.1 expression vector (Thermo Fisher Scientific; ref. 22).

MiR *xCT* expression plasmid was constructed using BLOCK-iT Pol II miR RNAi Expression vector kits (Thermo Fisher Scientific). *xCT* miRNA oligo sequence were: sense, 5′-AGAUAUGCAUC-GUCCUUUCAA-3′ and anti-sense, 5′-UUGAAAGGACGAUG-CAUAUCU-3′.

Dual-luciferase reporter assay

The reporter vector (100 ng) and the expression vector (2,000 ng) were reverse transfected with Lipofectamine 3000 (Thermo Fisher Scientific) into colon 26 cells (6-well plate; 2.5×10^5 cells/well). To correct for the variations in transfection efficiency, 0.5 ng phRL-TK vector (Promega) were cotransfected in all experiments. Total amount of DNA per well was adjusted by adding pcDNA3.3 vector (Thermo Fisher Scientific). Following the transfection, after 24 hours, Firefly and *Renilla* luciferase activity was analyzed using the Dual Luciferase Reporter Assay System (Promega). In each sample, the luciferase activity determined for the reporter plasmid was normalized to *Renilla* luciferase activity.

Circadian clock synchronization

Colon 26 cells were seeded at a density 2.5×10^5 cell/well in 6-well plates. After 24 hours, the medium was replaced with serum-free medium. Twelve hours later, the cells were stimulated with 50% FBS RPMI 1640, and after the additional 2 hours, the medium was removed and cells were washed 2 times and incubated in RPMI 1640 with 5% FBS.

Colon 26 cells were transfected with si-Bmal1, si-Clock, or negative control siRNA. The transfected cells were seeded at a density of 2.5×10^5 cell/well in 6-well plates. After 24 hours, the medium was replaced with serum-free medium, and after the additional 12 hours, the transfected cells were stimulated with 50% FBS RPMI 1640. Two hours later, medium was removed and cells were washed 2 times and incubated in RPMI 1640 with 5% FBS.

Western blotting analysis

Total proteins were extracted using T-PER Tissue Protein Extraction Reagent (Thermo Fisher Scientific). Membrane proteins were extracted using the Mem-PER Plus Membrane Protein Extraction Kit (Thermo Fisher Scientific). The protein concentration was determined using the BCA Protein Assay Kit (Thermo Fisher Scientific). Lysate samples were separated on sodium dodecyl sulfate-polyacrylamide gels and transferred to polyvinylidene difluoride membranes. The membranes were incubated with antibodies against Bmal1 (Santa Cruz Biotechnology), Clock (Santa Cruz Biotechnology), xCT (Abcam), β-actin (Cell Signaling Technology), and Na,K-ATPase (Cell Signaling Technology). Immunocomplexes were detected by incubating the samples with horseradish peroxidase–conjugated secondary antibodies and were visualized using ImmunoStar Zeta (Wako Pure Chemical Industries, Ltd.). The membranes were photographed using Polaroid-type film or an Image Quant LAS-4000 (Fujifilm). The mean value of the lowest gene expression levels or that obtained in the si-control group was set to 1.

Chromatin immunoprecipitation assay

Tumors were crosslinked using 10% formaldehyde in PBS at 25°C for 10 minutes. Each crosslinked sample was sonicated by Covaris Model S1 (Covaris) and incubated with antibodies against Bmal1 and Clock (1:1). Chromatin/antibody complexes

Published OnlineFirst October 16, 2017; DOI: 10.1158/0008-5472.CAN-17-0720

were extracted using IP Kit Dynabeads Protein G (Veritas). DNA was isolated from the immunoprecipitates and analyzed by PCR using the following sequences targeting the E-box of the *xCT* promoter region: 5′-TCAGGAATCTGACCTTCTTGGC-3′ and 5′-ACTGTCTTCCTCCTGCTTTCTG-3′. Data were normalized to the input control, which consisted of PCR reactions performed on crosslinked chromatin before immunoprecipitation. Quantitative data were obtained as the ratio to input DNA. The mean value obtained at 5:00 was set to 1.

Determination of the anticancer effects

Sulfasalazine (Wako Pure Chemical Industries, Ltd.) solutions (10 mg/mL) were prepared every day in 0.1 N NaOH subsequently adjusted with 1.0 N HCl to a pH of about 8, according to a previously reported method (23). Colon 26 cells were implanted into the right footpad of BALB/c mice. One day after inoculation, sulfasalazine (500 mg/kg) was intraperitoneally administered to colon 26 tumor–bearing mice at 17:00 or 5:00 once per day for 14 days, and 0.9% NaCl solution was administered to the control group. One day after inoculation, oxaliplatin (1 mg/kg) was intravenously administered to colon 26 tumor–bearing mice at 17:00 or 5:00 every 3 days, whereas 5% glucose solution was administered to the control group. The length, width, and height of tumors were measured using digital calipers every 3 days throughout the duration of the experiment.

Detection of intracellular GSH

Tumors were extracted from colon 26 tumor–bearing mice 1 day after sulfasalazine treatment. GSH and GSH/oxidized glutathione (GSSG) ratio was determined using the GSSG/GSH Quantification Kit (Dojindo Molecular Technologies, Inc.). Protein concentration was determined using the BCA Protein Assay Kit (Thermo Fisher Scientific).

Determination of the sulfasalazine concentration by liquid chromatography coupled with tandem mass spectrometry (LC/MS/MS)

Blood samples were obtained from the mouse hearts at 0.5, 1, and 3 hours after a single administration of sulfasalazine (500 mg/kg) at 17:00 or 5:00. Whole blood was allowed to clot, and sera were collected by centrifugation at 3,000 × *g* for 15 minutes. After the addition of internal standard (probenecid), serum samples were deproteinized with methanol and centrifuged at 20,500 × *g* for 5 minutes. The supernatants were allowed to evaporate, and the samples were dissolved in methanol and passed through a microporous membrane filter (Millex-GV 0.22-μm filters, Millipore Corp.). Samples were analyzed using a LC/MS/MS system, an ACQUITY ultra performance liquid chromatograph (UPLC) system (Waters), and an ACQUITY Triple Quadrupole Detector (Waters). Quantitation was performed by MRM in the negative ion mode. Chromatographic separation was performed at 35°C using an ACQUITY UPLC BEH C18 Column (1.7 μm, 2.1 mm × 100 mm, 1/pkg, Waters) under gradient conditions at a flow rate of 0.3 mL/min. Mobile phases consisted of 1 mmol/L ammonium formate containing 0.1% formic acid and methanol (15:85 v/v). The mass transition was from m/z 397 to 197 for sulfasalazine and from m/z 284.1 to 240.3 for the internal standard.

Statistical analysis

The unpaired *t* test was used for the comparison between two groups. One-way ANOVA was used for multiple comparisons. The Scheffe test was used for *post hoc* comparisons. Differences between the groups with a *P* value of <0.05 were considered statistically significant.

Results

Bmal1/Clock transcriptional regulation of xCT expression

We investigated the binding sites of clock molecules such as E-box, PAR bZip–responsive elements, and retinoic orphan receptor responsive elements in the promoter sequence of xCT (between 10,000 bp upstream and the transcriptional start site), and identified the E-box (−2,716 bp), a Bmal1/Clock heterodimer response element, in this region (Fig. 1A). A previous report showed that sulfasalazine inhibits the growth of CSCs in colon cancer patients (21), and therefore, we used colon 26 cells. We performed *Bmal1* or *Clock* knockdown in colon 26 cells and investigated the changes in *xCT* expression. We confirmed that *Bmal1* and *Clock* knockdown leads to the reduction in Bmal1 and Clock levels, respectively (Fig. 1B). Bmal1 and Clock siRNA treatment led to a decrease in *xCT* levels compared with those in the control group (Fig. 1C, $P < 0.01$): si-Bmal1, by 55%; and si-Clock, by 85%. Furthermore, we constructed a luciferase reporter plasmid containing the E-box derived from the mouse *xCT* promoter and the mutated E-box (Fig. 1A). The dual-luciferase assay showed that the luciferase activity increased approximately 3-fold in cells cotransfected with *xCT*-Luc, *Bmal1*, and *Clock* compared with that in the control group (Fig. 1D, $P < 0.01$). In contrast to this, luciferase activity was not induced in cells carrying E-box–mutated vector (Fig. 1D).

Clock effects on xCT circadian rhythm

We performed *Bmal1* or *Clock* knockdown in serum-shocked colon 26 cells using siRNAs. The circadian rhythm in the expression of *xCT* was observed in serum-shocked colon 26 cells, with the lowest levels measured 24 hours after the serum treatment, whereas the highest levels were determined 36 hours after the serum treatment. In contrast, the levels of *Wee1*, a key regulator expressed at the G_2–M cell-cycle checkpoint, did not show circadian rhythm after serum treatment (Fig. 2A). *Bmal1* knockdown led to an approximately 40% reduction in the basal *xCT* expression, compared with that in control group ($P < 0.05$). However, *xCT* expression was induced in *Bmal1* knockdown and the control groups 36 hours after the serum treatment. In contrast to this, in the *Clock*-knockdown group, this increase in *xCT* expression was not observed 36 hours after the serum treatment. We confirmed that the levels of *Dbp*, a known clock-controlled gene we used as a control, fail to be induced by serum treatment in *Bmal1* or *Clock* knockdown cells (Fig. 2B).

Circadian expression of xCT in tumors

xCT expression levels in colon 26 cells were determined using qRT-PCR, and the expression of this gene showed a significant circadian rhythm in colon 26 tumors, with the highest levels observed at 17:00 and the lowest at 5:00 (Fig. 3A). We confirmed that *xCT* expression shows circadian rhythms in other cancer cells as well, including in S180 cells (Fig. 3B). In order to investigate how this circadian rhythm affects xCT protein expression in the membrane of colon 26 tumors, we used Western blotting. The

Published OnlineFirst October 16, 2017; DOI: 10.1158/0008-5472.CAN-17-0720

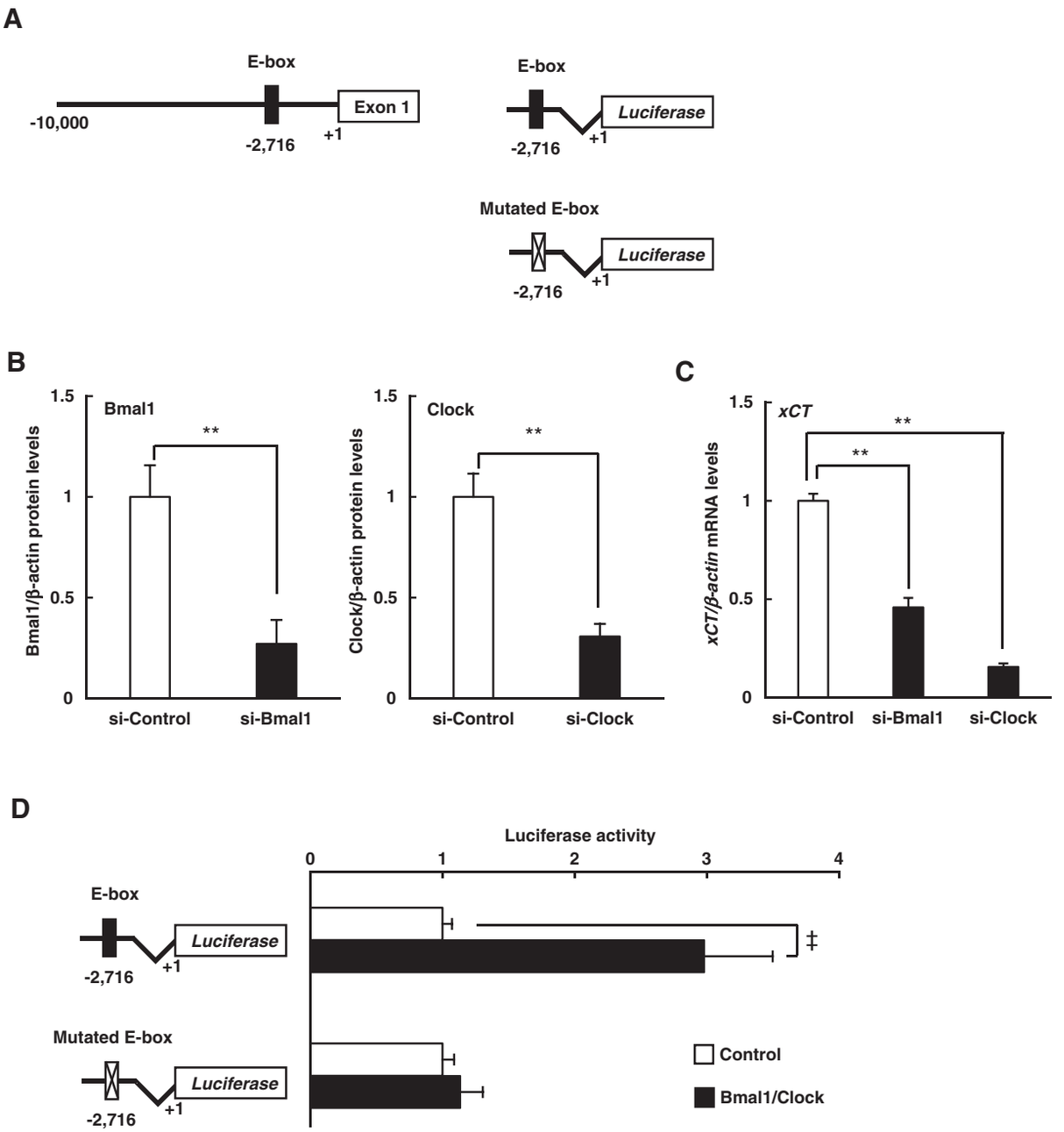

Figure 1.

Bmal1/Clock transcriptional regulation of *xCT* expression. **A,** Schematic representation of the mouse *xCT* promoter and *xCT* reporter genes. **B,** Effects of *Bmal1* or *Clock* knockdown on Bmal1 or Clock protein expression 48 hours after transfection. **, $P < 0.01$ (unpaired *t* test). **C,** Effect of *Bmal1* or *Clock* knockdown on *xCT* mRNA expression 48 hours after transfection. **, $P < 0.01$ (Scheffe test). **D,** Effect of *Bmal1* and *Clock* on transcriptional activity of *xCT*. ‡, $P < 0.01$ (unpaired *t* test). Data are represented as mean ± SD ($n = 3$ transfection experiments).

expression pattern of xCT membrane protein in colon 26 tumors showed significant circadian rhythm, with the highest levels observed at 21:00 and the lowest at 13:00 (Fig. 3C). We investigated the temporal binding of endogenous Bmal1/Clock to the E-box (–2,716 bp) in *xCT* promoter using chromatin immunoprecipitation assay. Endogenous Bmal1/Clock levels in colon 26 tumors were shown to be approximately 4-fold higher at 17:00 than at 5:00 (Fig. 3D, $P < 0.05$). In contrast, *xCT* promoters were not detected when normal IgG was used as the first antibody.

Published OnlineFirst October 16, 2017; DOI: 10.1158/0008-5472.CAN-17-0720

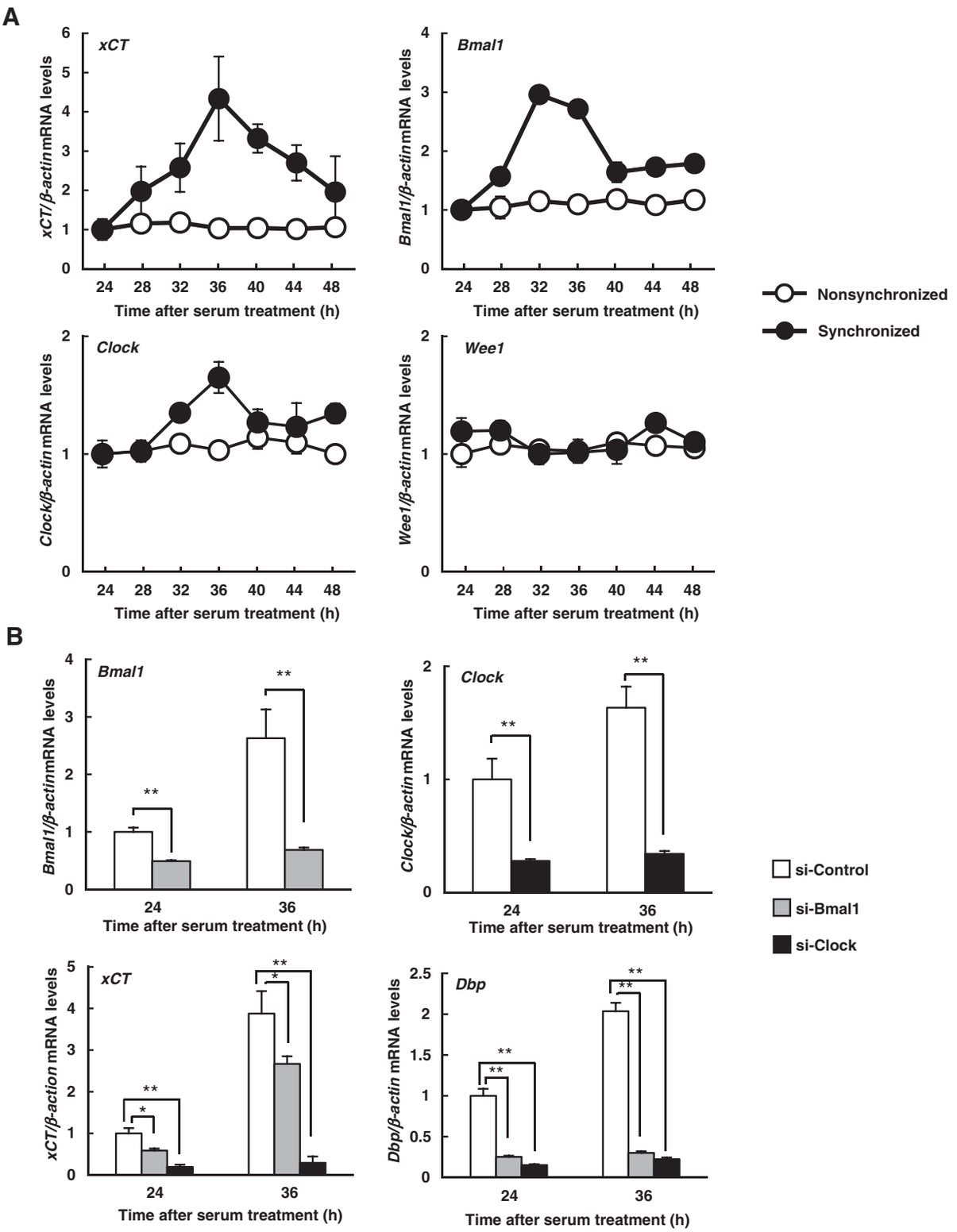

Figure 2.

Clock effects on *xCT* circadian rhythm. **A,** Temporal expression of *xCT, Bmal1, Clock,* and *Wee1* mRNA in nonsynchronized (ANOVA, *N.S.*) and serum-shocked (synchronized; ANOVA, *xCT,* $P < 0.01$; *Bmal1,* $P < 0.01$; *xCT,* $P < 0.01$; *Wee1, N.S.*) colon 26 cells ($n = 3$ cultures for each group). **B,** Effect of *Bmal1* and *Clock* knockdown on *Bmal1, Clock, xCT*, and *Dbp* mRNA expression in serum-shocked colon 26 cells ($n = 3$ transfection experiments). *, $P < 0.05$; **, $P < 0.01$ (unpaired *t* test or Scheffe test). Data are represented as mean ± SD.

Published OnlineFirst October 16, 2017; DOI: 10.1158/0008-5472.CAN-17-0720

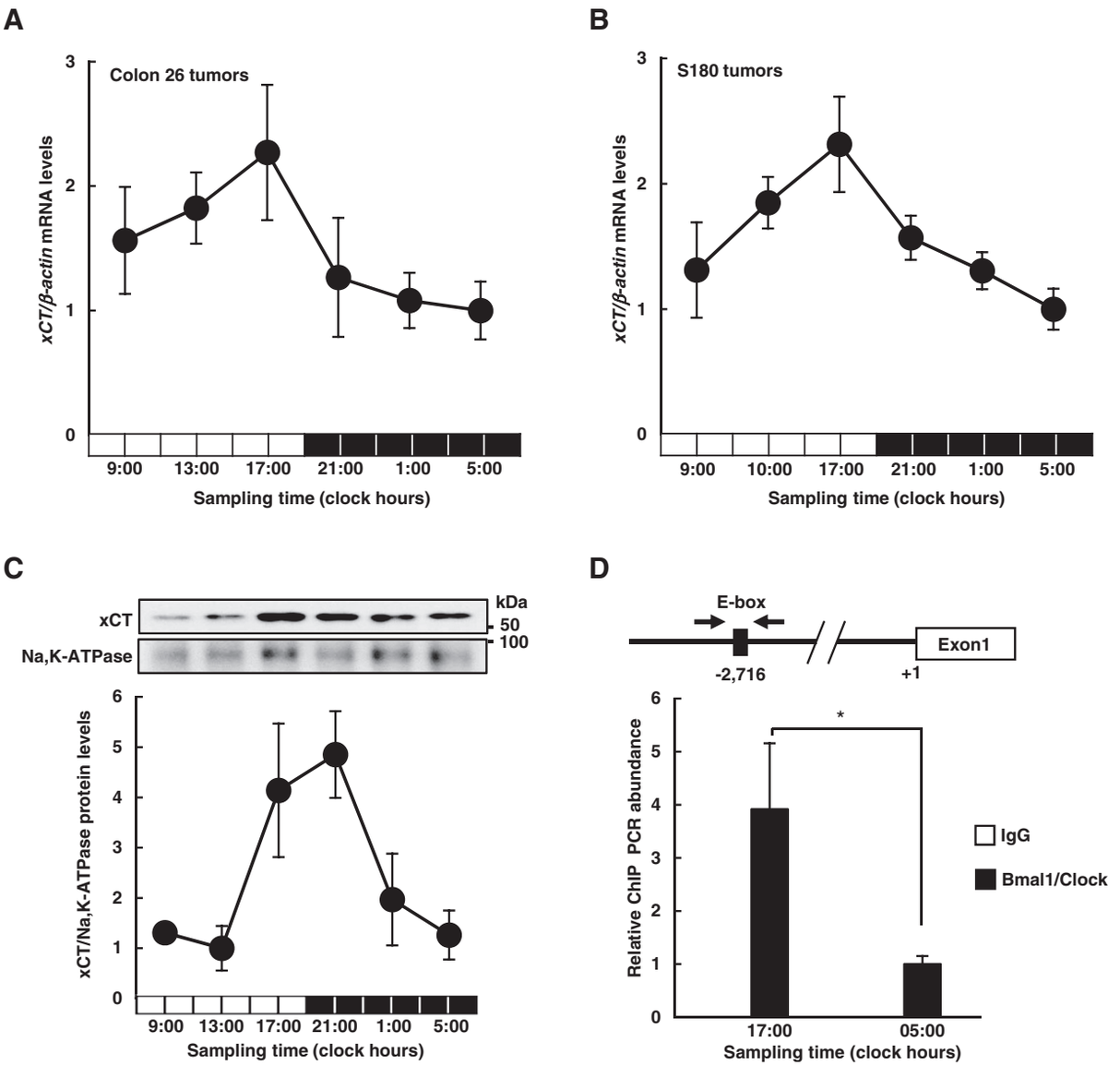

Figure 3.

Circadian expression of xCT in tumor masses. **A,** Temporal expression profiles of *xCT* mRNA in the implanted colon 26 tumors ($n = 6$ mice for each group), $P < 0.01$ (ANOVA). **B,** Temporal expression profiles of *xCT* mRNA in the implanted S180 tumors ($n = 6$ mice for each group), $P < 0.01$ (ANOVA). **C,** Temporal expression profiles of xCT membrane proteins in the implanted colon 26 tumors ($n = 3$ mice for each group), $P < 0.01$ (ANOVA). **D,** Temporal binding profiles of Bmal1/Clock or control IgG to E-box (−2,716 bp) in the mouse *xCT* promoter in the implanted colon 26 tumors ($n = 3$ mice for each group). Control IgG was not detected at this scale. **, $P < 0.01$ (unpaired t test). Data are represented as mean ± SD.

Sulfasalazine dosing time affects tumor growth inhibition

xCT expression was shown to be higher between 17:00 and 21:00 and lower between 5:00 and 9:00 in colon 26 tumors (Fig. 3). To explore the effects of sulfasalazine dosing time on its antitumor effects, sulfasalazine (500 mg/kg) was administered at 17:00 or 5:00 to colon 26 tumor–bearing mice. The tumor volume in mice treated with sulfasalazine at 17:00 significantly decreased by more than 60% compared with that of the mice treated at 5:00 (Fig. 4, $P < 0.05$). A previous report demonstrated that sulfasalazine shows dose-dependent anticancer effects (24). To verify the association between sulfasalazine dosing time and its antitumor effects, sulfasalazine concentration in blood was determined by LC/MS/MS after a single administration of sulfasalazine (500 mg/kg) at 17:00 or 5:00. Sulfasalazine levels in blood at 0.5 hours after sulfasalazine administration were shown to be significantly higher in mice that received the investigated drug at 5:00 (Fig. 5, $P < 0.01$).

In order to determine the effects of the circadian rhythm of *xCT* expression and sulfasalazine dosing time on its antitumor activity, we performed *ClockΔ19* and *xCT* knockdown in colon 26 cells.

Published OnlineFirst October 16, 2017; DOI: 10.1158/0008-5472.CAN-17-0720

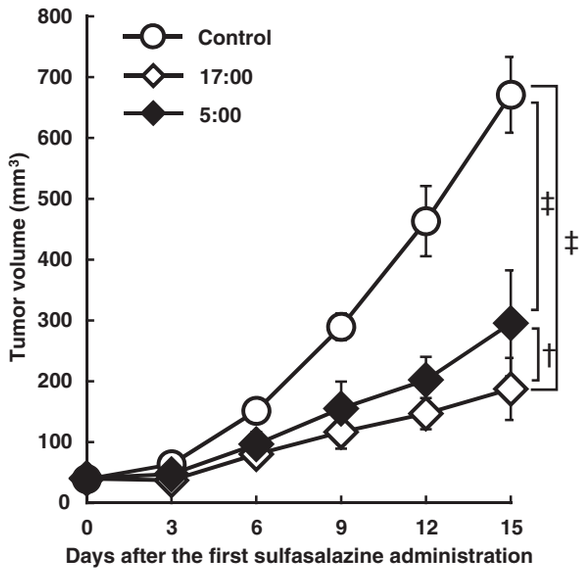

Figure 4.
Effect of dosing time of sulfasalazine on tumor growth in colon 26 tumor–bearing mice. Colon 26 tumor–bearing mice were intraperitoneally administered sulfasalazine (500 mg/kg) at 17:00 or 5:00 once per day for 14 days. Data are represented as mean ± SD ($n = 6$ mice for each group). †, $P < 0.05$; ‡, $P < 0.01$ (Scheffe test).

xCT expression failed to exhibit circadian rhythm in *ClockΔ19* and *xCT* knockdown colon 26 tumors (Fig. 6A and B). Sulfasalazine (500 mg/kg) was administered at 17:00 or 5:00 to *ClockΔ19* and *xCT* knockdown colon 26 tumor–bearing mice. The tumor volume in mice treated with sulfasalazine at 17:00 did not decrease significantly compared with that in the mice treated at 5:00 (Fig. 6C and D).

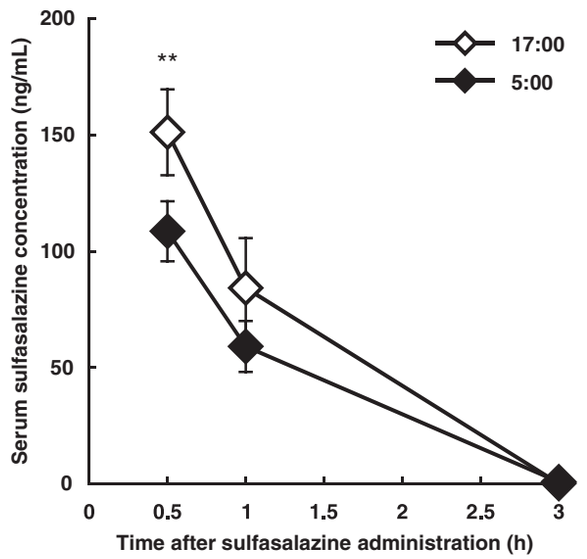

Figure 5.
Effect of dosing time of sulfasalazine on serum sulfasalazine concentration in mice. BALB/c mice were intraperitoneally administered a single dose of sulfasalazine (500 mg/kg) at 17:00 or 5:00. Data are represented as mean ± SD ($n = 5$ mice for each group). *, $P < 0.05$ (unpaired t test).

Sulfasalazine dosing time affects combination therapy

In order to determine the effects of the sulfasalazine dosing time on GSH metabolism, we determined GSH levels and GSH/GSSG ratio in colon 26 tumors after sulfasalazine treatment. GSH levels in mice treated with sulfasalazine at 17:00 significantly decreased by approximately 50% compared with those measured in mice treated at 5:00 (Fig. 7A; $P < 0.01$). Sulfasalazine administration led to a decrease in GSH/GSSG ratio, which is a marker of oxidative stress and toxicity, compared with that in the control group: if treated at 17:00, by more than 70% ($P < 0.01$); if treated at 5:00, by 50% ($P < 0.01$). In addition, GSH/GSSG ratio in mice treated with sulfasalazine at 17:00 decreased by 50% compared with that measured in mice treated at 5:00 (Fig. 7B; $P = 0.055$). To explore the effects of sulfasalazine dosing time on the anticancer effects of other anticancer drugs, oxaliplatin (1 mg/kg) was administered at 17:00 and 5:00 to the sulfasalazine-treated colon 26 tumor–bearing mice. The tumor volume in mice treated with sulfasalazine and oxaliplatin combination at 17:00 significantly decreased by approximately 40% compared with that in the mice treated with sulfasalazine at 17:00 (Fig. 7C, $P < 0.05$). In contrast to this, in the mice treated with sulfasalazine and oxaliplatin combination at 5:00, these sulfasalazine-induced oxaliplatin anticancer effects were not observed (Fig. 7D).

Discussion

Recently, xCT inhibitors have been the focus of novel anticancer agent development. CD44 and CD44 variant isoforms (CD44v) stabilize xCT and induce xCT expression and antioxidant activity in cancer cells (11, 19, 21). Sulfasalazine, xCT inhibitor, reduces CD44v expression and cell proliferation. Therefore, xCT inhibitors may induce oxidative stress in cancer cells and inhibit cell proliferation (18–20, 23). CD44 and CD44v are CSC markers, and the regulation of xCT by CD44 and CD44v has recently attracted attention (25–27). However, relatively little is known about the mechanisms of *xCT* transcriptional regulation.

We demonstrated that Bmal1 and Clock represent *xCT* transcriptional regulators. Bmal1 and Clock form a heterodimer, which binds to the E-box located in the promoter of the target genes, thereby inducing their expression (2–4). In this study, we found only one E-box located in the *xCT* promoter and showed that *Bmal1* and *Clock* knockdown leads to the reduction in *xCT* levels, and Bmal1 and Clock coexpression increased *xCT*-luciferase activity. These results demonstrate that *xCT* expression is regulated by Bmal1/Clock heterodimer at the transcriptional level. In addition, we demonstrated that Bmal1 and Clock regulate the circadian rhythm of *xCT* expression. The treatment with high-serum concentrations induces robust circadian rhythms in the cultured cells (28, 29). In addition, this treatment also affects cell-cycle synchronization (30). In this study, *Wee1* expression did not show circadian rhythm between 24 and 48 hours after serum treatment, and we confirmed that *Clock* genes directly affect *xCT* levels without cell-cycle effects in serum-shocked colon 26 cells. Furthermore, we demonstrated that *Bmal1* knockdown did not suppress the induction of *xCT* expression 36 hours after the serum treatment, whereas the knockdown of *Clock* did. xCT mRNA and membrane protein expression were shown to be higher between 17:00 and 21:00 and lower between 5:00 and 9:00 in colon 26

Published OnlineFirst October 16, 2017; DOI: 10.1158/0008-5472.CAN-17-0720

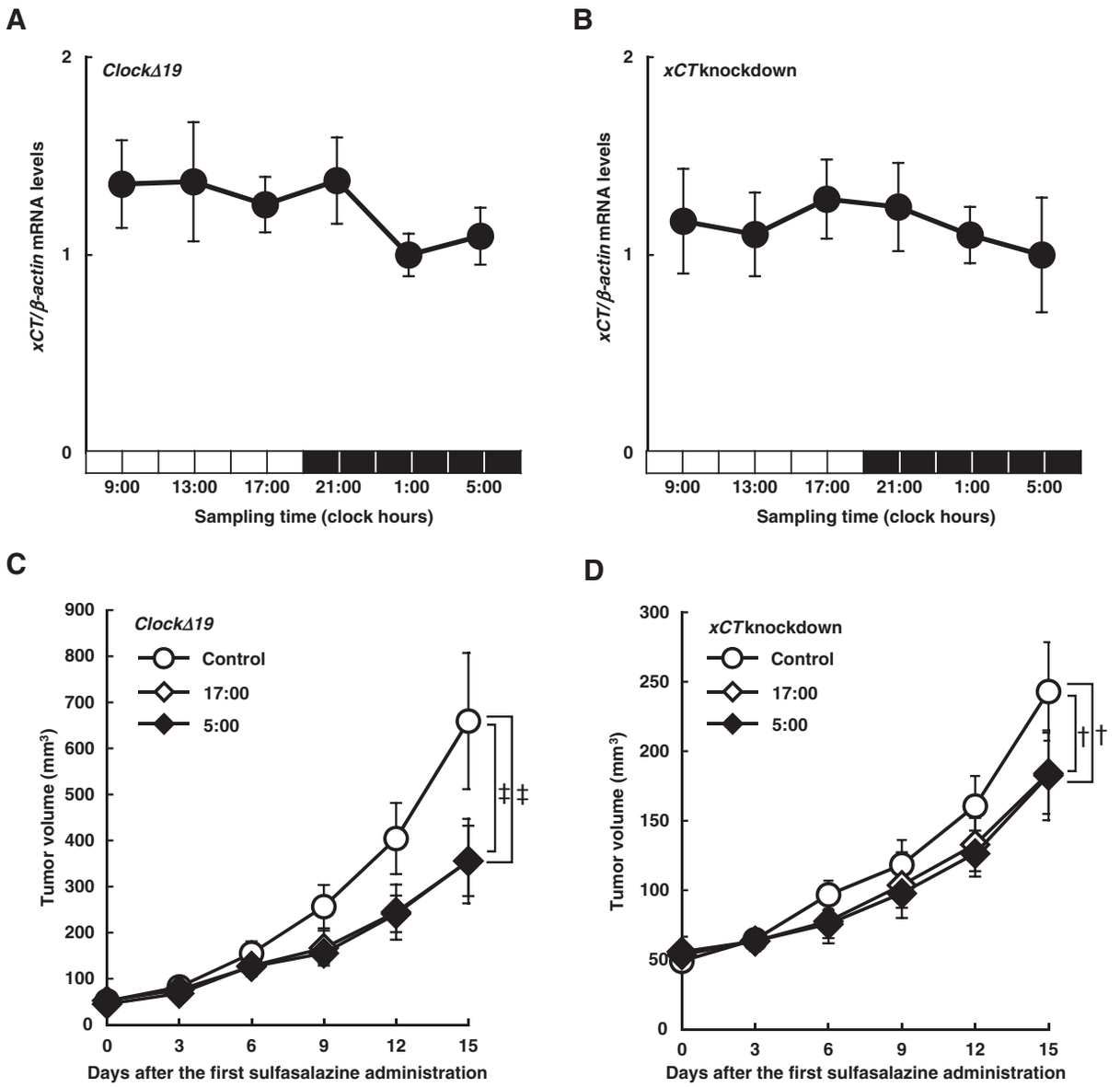

Figure 6.

Effect of circadian rhythm of *xCT* expression on anticancer effects of sulfasalazine. **A,** Temporal expression profiles of *xCT* mRNA in the implanted *ClockΔ19* colon 26 tumors (*N.S.,* ANOVA; $n = 3$ mice for each group). **B,** Temporal expression profiles of *xCT* mRNA in the implanted *xCT* knockdown colon 26 tumors (*N.S.,* ANOVA; $n = 3$ mice for each group). **C,** Effect of dosing time of sulfasalazine on the tumor growth in *ClockΔ19* colon 26 tumor–bearing mice. *ClockΔ19* colon 26 tumor–bearing mice were intraperitoneally administered sulfasalazine (500 mg/kg) at 17:00 or 5:00 once per day for 14 days ($n = 6$ mice for each group). †, $P < 0.05$; ‡, $P < 0.01$ (Scheffe test). **D,** Effect of dosing time of sulfasalazine on the tumor growth in *xCT* knockdown colon 26 tumor–bearing mice. *xCT* knockdown colon 26 tumor–bearing mice were intraperitoneally administered sulfasalazine (500 mg/kg) at 17:00 or 5:00 once per day for 14 days ($n = 6$ mice for each group). †, $P < 0.05$ (Scheffe test). Data are represented as mean ± SD.

tumors, whereas it was demonstrated in our previous report that Clock protein expression is increased between 17:00 and 21:00 as well (22). Therefore, taken together, these results indicate that Clock may represent the main regulator of the circadian rhythm of *xCT* expression.

Iron is an essential material for DNA synthesis during cell proliferation; however, iron overload induces oxidative stress, and the increase in xCT levels induces the cells to enter the S phase of the cell cycle (31). On the other hand, the inhibition of iron metabolism reduces cystine and GSH levels (32). We previously demonstrated that iron metabolism exhibited circadian rhythms, whereas iron levels were shown to be higher at 21:00 in the colon 26 tumors (22, 33). Here, we showed that the expression of xCT increases between 17:00 and 21:00, suggesting that the circadian rhythm of xCT expression is involved in the protection from the oxidative stress and in the cell cycle through iron metabolism.

Published OnlineFirst October 16, 2017; DOI: 10.1158/0008-5472.CAN-17-0720

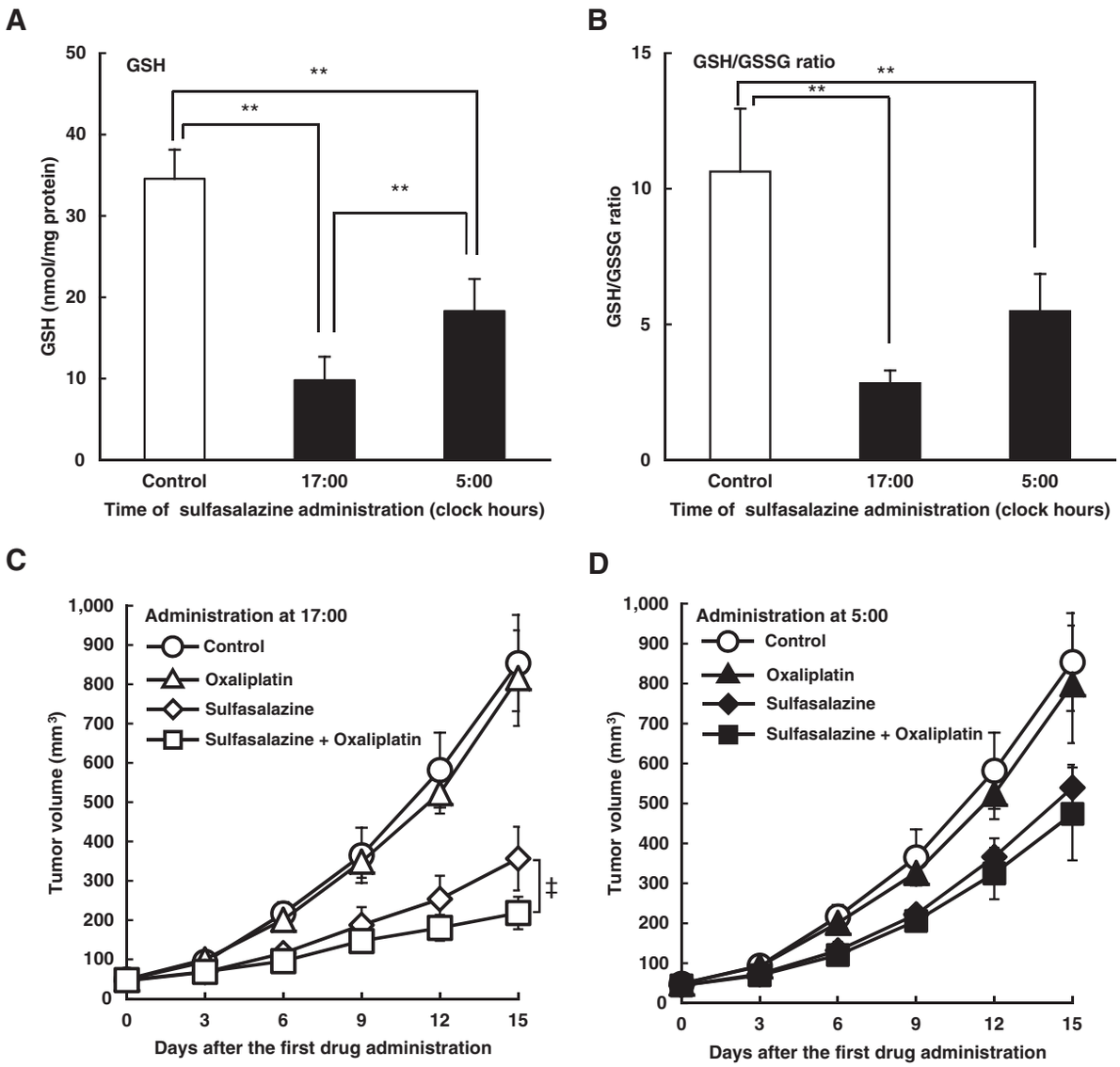

Figure 7.

Effect of dosing time of sulfasalazine on combination therapy in colon 26 tumor–bearing mice. **A,** Effect of dosing time of sulfasalazine on GSH levels in the implanted colon 26 tumors. **B,** Effect of dosing time of sulfasalazine on GSH/GSSG ratio in the implanted colon 26 tumors. Colon 26 tumor–bearing mice were intraperitoneally administered sulfasalazine (500 mg/kg) at 17:00 or 5:00 once per day for 14 days. *, $P < 0.05$; **, $P < 0.01$ (Scheffe test). **C,** Effect of dosing time of sulfasalazine on sensitivity of oxaliplatin in the implanted colon 26 tumors. Colon 26 tumor–bearing mice were intraperitoneally administered sulfasalazine (500 mg/kg) at 17:00 once per day for 14 days and were intravenously administered with oxaliplatin (1 mg/kg) at 17:00 every 3 days. ‡, $P < 0.01$ (unpaired t test). **D,** Effect of dosing time of sulfasalazine on sensitivity of oxaliplatin in the implanted colon 26 tumors. Colon 26 tumor–bearing mice were intraperitoneally administered sulfasalazine (500 mg/kg) at 5:00 once per day for 14 days and were intravenously administered with oxaliplatin (1 mg/kg) at 5:00 every 3 days (*N.S.*, unpaired t test, Sulfasalazine vs. Sulfasalazine + Oxaliplatin). Data are represented as mean ± SD ($n = 6$ mice for each group).

Breast cancer resistance protein (BCRP/ABCG2) affects sulfasalazine pharmacokinetics (34). *Bcrp* expression showed circadian rhythms, and sulfasalazine levels in the blood showed the dosing time-dependent difference in mice that received sulfasalazine orally (35). Sulfasalazine is mainly eliminated by bile, and because mice are nocturnal animals and are active in the dark, blood fluid and bile secretion increase in the dark. Therefore, these factors may underlie the dosing time-dependent variation in sulfasalazine pharmacokinetics. Sulfasalazine is an anti-inflammatory and antirheumatic drug, and previous studies showed that it inhibits tumor growth and that its anticancer effects are mediated through the inhibition of xCT (18–21). Sulfasalazine is metabolized by colonic bacteria, producing 5-aminosalicylic acid and sulfapyridine. By intraperitoneal administration of sulfasalazine, we demonstrated that its anticancer effects improve when it is administered during the period of increased xCT expression, ultimately leading to the reduction in the tumor volume and the inhibition of GSH metabolism. Sulfasalazine administration at

Published OnlineFirst October 16, 2017; DOI: 10.1158/0008-5472.CAN-17-0720

17:00 failed to reduce the tumor growth in *ClockΔ19* and *xCT* knockdown cells, which also showed no significant circadian rhythms in *xCT* expression. Therefore, chronomodulated chemotherapy using xCT inhibitors may lead to an improvement in the anticancer effects, although the results obtained here indicate that this may be due to the effects on the pharmacokinetic parameters of sulfasalazine.

Previous studies suggested that the anticancer effects of various drugs are induced by sulfasalazine and an inhibitor of GSH metabolism (18, 19). GSH levels were shown to decrease after sulfasalazine administration during the period of increased xCT expression. Oxaliplatin is used for the treatment of colorectal cancer, and therefore, we used oxaliplatin in this combination study. In addition, in order to elucidate the sulfasalazine-induced anticancer effects, a low-dose oxaliplatin (1 mg/kg), which did not show anticancer effects, was administered to the mice treated with sulfasalazine. Oxaliplatin combination led to the tumor growth inhibition in mice treated with sulfasalazine at 17:00 when xCT increased. This suggested the chronomodulated chemotherapy using xCT inhibitors may enhance anticancer effects of other drugs.

NAD(H) and NADP(H) are involved in the protection from oxidative stress, and NADP(H) plays essential roles in the GSH metabolism (36–38). xCT inhibition affects GSH expression and NADPH oxidase activity (39). Previous studies showed that NAD(H) and NADP(H) can affect DNA-binding activity of Bmal1/Clock, and NAD(H) and NADP(H) levels vary in the cells *in vitro* with serum treatment and tissues (40–43). Taken together, the results obtained in this study indicate that xCT inhibitors affect circadian rhythms through GSH metabolism, improving the anticancer effects.

In recent years, chronomodulated chemotherapeutic strategies based on the optimal drug pharmacokinetic and pharmacodynamics parameters have been developed. Here, we demonstrated that the expression of xCT is controlled by *Clock* gene, which results in the observed circadian rhythm in xCT expression in colon 26 cells. The alterations in xCT expression were shown to lead to the dosing time-dependent variations in anticancer effects of sulfasalazine. These findings strongly suggest that the anticancer efficacy of xCT inhibitors may be improved by the modulation of drug administration time. Our study elucidated xCT transcriptional regulation in cancer cells, which may help design improved anticancer treatment strategies in the future.

Disclosure of Potential Conflicts of Interest

No potential conflicts of interest were disclosed.

Authors' Contributions

Conception and design: F. Okazaki, N. Matsunaga, H. To
Development of methodology: F. Okazaki
Acquisition of data (provided animals, acquired and managed patients, provided facilities, etc.): F. Okazaki, N. Matsunaga, K. Suzuki, T. Nakao
Analysis and interpretation of data (e.g., statistical analysis, biostatistics, computational analysis): F. Okazaki, M. Kutsukake
Writing, review, and/or revision of the manuscript: F. Okazaki, S. Fukumori
Administrative, technical, or material support (i.e., reporting or organizing data, constructing databases): F. Okazaki, K. Hamamura, H. Okazaki, S. Fukumori
Study supervision: F. Okazaki, Y. Tsuji, H. To

Grant Support

This work was supported by the Life Science Research Center, University of Toyama, and the Platform Project for Supporting Drug Discovery and Life Science Research [Basis for Supporting Innovative Drug Discovery and Life Science Research (BINDS)] from Japan Agency for Medical Research and Development (AMED). This study was also supported by the Japan Society for the Promotion of Science (JSPS) KAKENHI grant numbers JP26860097, JP30756466, and 15K19163.

The costs of publication of this article were defrayed in part by the payment of page charges. This article must therefore be hereby marked *advertisement* in accordance with 18 U.S.C. Section 1734 solely to indicate this fact.

Received March 16, 2017; revised June 22, 2017; accepted October 4, 2017; published OnlineFirst October 16, 2017.

References

1. Stephan FK, Zucker I. Circadian rhythms in drinking behavior and locomotor activity of rats are eliminated by hypothalamic lesions. Proc Nat Acad Sci U S A 1972;69:1583–6.
2. Alvarez JD, Sehgal A. Circadian rhythms: finer clock control. Nature 2002;419:798–9.
3. Kume K, Zylka MJ, Sriram S, Shearman LP, Weaver DR, Jin X, et al. mCRY1 and mCRY2 are essential components of the negative limb of the circadian clock feedback loop. Cell 1999;98:193–205.
4. Gekakis N, Staknis D, Nguyen HB, Davis FC, Wilsbacher LD, King DP, et al. Role of the CLOCK protein in the mammalian circadian mechanism. Science (New York, NY) 1998;280:1564–9.
5. Michael AK, Harvey SL, Sammons PJ, Anderson AP, Kopalle HM, Banham AH, et al. Cancer/testis antigen PASD1 silences the circadian clock. Mol Cell 2015;58:743–54.
6. Panda S, Hogenesch JB, Kay SA. Circadian rhythms from flies to human. Nature 2002;417:329–35.
7. Young MW, Kay SA. Time zones: a comparative genetics of circadian clocks. Nat Rev Genet 2001;2:702–15.
8. Dallmann R, Okyar A, Levi F. Dosing-time makes the poison: circadian regulation and pharmacotherapy. Trends Mol Med 2016;22:430–45.
9. Fu L, Kettner NM. The circadian clock in cancer development and therapy. Prog Mol Biol Transl Sci 2013;119:221–82.
10. Kelleher FC, Rao A, Maguire A. Circadian molecular clocks and cancer. Cancer Lett 2014;342:9–18.
11. Lewerenz J, Hewett SJ, Huang Y, Lambros M, Gout PW, Kalivas PW, et al. The cystine/glutamate antiporter system x(c)(-) in health and disease: from molecular mechanisms to novel therapeutic opportunities. Antioxid Redox Signal 2013;18:522–55.
12. Kato S, Negishi K, Mawatari K, Kuo CH. A mechanism for glutamate toxicity in the C6 glioma cells involving inhibition of cystine uptake leading to glutathione depletion. Neuroscience 1992;48:903–14.
13. Tew KD.Glutathione-associated enzymes in anticancer drug resistance. Cancer Res 1994;54:4313–20.
14. Zhang Y, Martin SG. Redox proteins and radiotherapy. Clin Oncol 2014;26:289–300.
15. Dusre L, Mimnaugh EG, Myers CE, Sinha BK. Potentiation of doxorubicin cytotoxicity by buthionine sulfoximine in multidrug-resistant human breast tumor cells. Cancer Res 1989;49:511–5.
16. Chen G, Waxman DJ. Role of cellular glutathione and glutathione S-transferase in the expression of alkylating agent cytotoxicity in human breast cancer cells. Biochem Pharmacol 1994;47:1079–87.
17. Huang Y, Dai Z, Barbacioru C, Sadee W. Cystine-glutamate transporter SLC7A11 in cancer chemosensitivity and chemoresistance. Cancer Res 2005;65:7446–54.
18. Yoshikawa M, Tsuchihashi K, Ishimoto T, Yae T, Motohara T, Sugihara E, et al. xCT inhibition depletes CD44v-expressing tumor cells that are resistant to EGFR-targeted therapy in head and neck squamous cell carcinoma. Cancer Res 2013;73:1855–66.

Published OnlineFirst October 16, 2017; DOI: 10.1158/0008-5472.CAN-17-0720

19. Ishimoto T, Nagano O, Yae T, Tamada M, Motohara T, Oshima H, et al. CD44 variant regulates redox status in cancer cells by stabilizing the xCT subunit of system xc(-) and thereby promotes tumor growth. Cancer Cell 2011;19:387–400.
20. Timmerman LA, Holton T, Yuneva M, Louie RJ, Padro M, Daemen A, et al. Glutamine sensitivity analysis identifies the xCT antiporter as a common triple-negative breast tumor therapeutic target. Cancer Cell 2013;24:450–65.
21. Seishima R, Okabayashi K, Nagano O, Hasegawa H, Tsuruta M, Shimoda M, et al. Sulfasalazine, a therapeutic agent for ulcerative colitis, inhibits the growth of CD44v9(+) cancer stem cells in ulcerative colitis-related cancer. Clin Res Hepatol Gastroenterol 2016;40:487–93.
22. Okazaki F, Matsunaga N, Okazaki H, Azuma H, Hamamura K, Tsuruta A, et al. Circadian clock in a mouse colon tumor regulates intracellular iron levels to promote tumor progression. J Biol Chem 2016;291:7017–28.
23. Gout PW, Buckley AR, Simms CR, Bruchovsky N. Sulfasalazine, a potent suppressor of lymphoma growth by inhibition of the x(c)- cystine transporter: a new action for an old drug. Leukemia 2001;15:1633–40.
24. Gout PW, Simms CR, Robertson MC. In vitro studies on the lymphoma growth-inhibitory activity of sulfasalazine. Anticancer Drugs 2003;14:21–9.
25. Orian-Rousseau V, Ponta H. Perspectives of CD44 targeting therapies. Arch Toxicol 2015;89:3–14.
26. Nagano O, Okazaki S, Saya H. Redox regulation in stem-like cancer cells by CD44 variant isoforms. Oncogene 2013;32:5191–8.
27. Prochazka L, Tesarik R, Turanek J. Regulation of alternative splicing of CD44 in cancer. Cell Signal 2014;26:2234–9.
28. Balsalobre A, Damiola F, Schibler U. A serum shock induces circadian gene expression in mammalian tissue culture cells. Cell 1998;93:929–37.
29. Nagoshi E, Saini C, Bauer C, Laroche T, Naef F, Schibler U. Circadian gene expression in individual fibroblasts: cell-autonomous and self-sustained oscillators pass time to daughter cells. Cell 2004;119:693–705.
30. Casey T, Crodian J, Suarez-Trujillo A, Erickson E, Weldon B, Crow K, et al. CLOCK regulates mammary epithelial cell growth and differentiation. Am J Physiol Regul Integr Comp Physiol 2016;311:R1125–r34.
31. Chen RS, Song YM, Zhou ZY, Tong T, Li Y, Fu M, et al. Disruption of xCT inhibits cancer cell metastasis via the caveolin-1/beta-catenin pathway. Oncogene 2009;28:599–609.
32. Lall MM, Ferrell J, Nagar S, Fleisher LN, McGahan MC. Iron regulates L-cystine uptake and glutathione levels in lens epithelial and retinal pigment epithelial cells by its effect on cytosolic aconitase. Invest Ophthalmol Visual Sci 2008;49:310–9.
33. Okazaki F, Matsunaga N, Okazaki H, Utoguchi N, Suzuki R, Maruyama K, et al. Circadian rhythm of transferrin receptor 1 gene expression controlled by c-Myc in colon cancer-bearing mice. Cancer Res 2010; 70:6238–46.
34. Zaher H, Khan AA, Palandra J, Brayman TG, Yu L, Ware JA. Breast cancer resistance protein (Bcrp/abcg2) is a major determinant of sulfasalazine absorption and elimination in the mouse. Mol Pharm 2006;3:55–61.
35. Hamdan AM, Koyanagi S, Wada E, Kusunose N, Murakami Y, Matsunaga N, et al. Intestinal expression of mouse Abcg2/breast cancer resistance protein (BCRP) gene is under control of circadian clock-activating transcription factor-4 pathway. J Biol Chem 2012;287:17224–31.
36. Thelander L, Reichard P. Reduction of ribonucleotides. Annu Rev Biochem 1979;48:133–58.
37. Benhar M, Shytaj IL, Stamler JS, Savarino A. Dual targeting of the thioredoxin and glutathione systems in cancer and HIV. J Clin Invest 2016; 126:1630–9.
38. Tedeschi PM, Bansal N, Kerrigan JE, Abali EE, Scotto KW, Bertino JR. NAD+ kinase as a therapeutic target in cancer. Clin Cancer Res 2016;22:5189–95.
39. Dai L, Cao Y, Chen Y, Parsons C, Qin Z. Targeting xCT, a cystine-glutamate transporter induces apoptosis and tumor regression for KSHV/HIV-associated lymphoma. J Hematol Oncol 2014;7:30.
40. Rutter J, Reick M, Wu LC, McKnight SL. Regulation of clock and NPAS2 DNA binding by the redox state of NAD cofactors. Science (New York, NY) 2001;293:510–4.
41. Nakahata Y, Sahar S, Astarita G, Kaluzova M, Sassone-Corsi P. Circadian control of the NAD+ salvage pathway by CLOCK-SIRT1. Science (New York, NY) 2009;324:654–7.
42. Ramsey KM, Yoshino J, Brace CS, Abrassart D, Kobayashi Y, Marcheva B, et al. Circadian clock feedback cycle through NAMPT-mediated NAD+ biosynthesis. Science (New York, NY) 2009;324:651–4.
43. O'Neill JS, Reddy AB. Circadian clocks in human red blood cells. Nature 2011;469:498–503.

Published OnlineFirst October 16, 2017; DOI: 10.1158/0008-5472.CAN-17-0720

Cancer Research
The Journal of Cancer Research (1916–1930) | The American Journal of Cancer (1931–1940)

AACR American Association for Cancer Research

Administering xCT Inhibitors Based on Circadian Clock Improves Antitumor Effects

Fumiyasu Okazaki, Naoya Matsunaga, Kengo Hamamura, et al.

Cancer Res 2017;77:6603-6613. Published OnlineFirst October 16, 2017.